

Generative Pretrained Embedding and Hierarchical Irregular Time Series Representation for Daily Living Activity Recognition

Damien Bouchabou^{a,*} and Sao Mai Nguyen^{b,**}

^aU2IS, ENSTA, IP Paris, France

^bFLOWERS, U2IS, ENSTA, IP Paris & Inria and IMT Atlantique Lab-STICC, UMR 6285
ORCID (Damien Bouchabou): <https://orcid.org/0000-0003-3623-3626>, ORCID (Sao Mai Nguyen):
<https://orcid.org/0000-0003-0929-0019>

Abstract. Within the evolving landscape of smart homes, the precise recognition of daily living activities using ambient sensor data stands paramount. This paper not only aims to bolster existing algorithms by evaluating two distinct pretrained embeddings suited for ambient sensor activations but also introduces a novel hierarchical architecture. We delve into an architecture anchored on Transformer Decoder-based pre-trained embeddings, reminiscent of the GPT design, and contrast it with the previously established state-of-the-art (SOTA) ELMo embeddings for ambient sensors. Our proposed hierarchical structure leverages the strengths of each pre-trained embedding, enabling the discernment of activity dependencies and sequence order, thereby enhancing classification precision. To further refine recognition, we incorporate into our proposed architecture an hour-of-the-day embedding. Empirical evaluations underscore the preeminence of the Transformer Decoder embedding in classification endeavors. Additionally, our innovative hierarchical design significantly bolsters the efficacy of both pre-trained embeddings, notably in capturing inter-activity nuances. The integration of temporal aspects subtly but distinctively augments classification, especially for time-sensitive activities. In conclusion, our GPT-inspired hierarchical approach, infused with temporal insights, outshines the SOTA ELMo benchmark.

1 Introduction

Recognizing and analyzing temporal event sequences is a fundamental challenge in artificial intelligence and data science, involving pattern identification in time-ordered observations. This task requires capturing short and long-term dependencies, handling irregular sampling, and accounting for noise and variability. Human Activity Recognition (HAR) in smart homes exemplifies this challenge. With the Internet of Things (IoT) advancements, homes are increasingly equipped with ambient sensors (e.g., motion, door open/close, temperature), with the outlook of offering services for improving the quality of daily life or health. HAR algorithms aim to recognize Activities of Daily Living (ADL) like cooking or sleeping from these sensor activations, forming the basis for health and well-being services. Deep learning has emerged as a leading approach in HAR due

to its proficiency in interpreting raw sensor data [10, 15, 23, 20]. However, challenges persist [3], including noisy, irregularly sampled data from battery-powered sensors, limited contextual information due to privacy concerns, and the complexity of ADLs involving variable-length actions with multilevel temporal dependencies. These factors strain traditional modeling methods.

To address long-term dependencies, hierarchical models like ontologies [11] and hidden Markov models [1] have been proposed. Recent deep learning paradigms offer single-level sequence models [14, 13, 19], but struggle with irregular time series and long-range contexts. Recurrent Neural Networks (RNN) and language models (ELMo [16], GPT-2 [17]) show promise but have limitations for longer-range contexts [4, 21].

This work tackles a multivariate non-Markovian irregular time series in the context of ADLs recognition into smart homes, by examining event timestamps, contextual encoding, and long-term dependency. Our approach combines: (1) attention mechanisms for discerning the importance of sensor signals across a whole sequence, (2) pre-trained generative transformer embeddings capturing sensor interrelations, (3) a hierarchical model emphasizing activity succession for long-horizon dependency, and (4) a temporal encoding model to harness the timing of events.

We propose a multi-timescale architecture for wider temporal dependency, contextualizing non-Markov time series events.

Code available at: <https://github.com/dbouchabou/Generative-Pretrained-Embedding-and-Hierarchical-Representation-to-Unlock-ADL-Rhythm-in-Smart-Homes.git>.

Annexes available at: <https://github.com/dbouchabou/Generative-Pretrained-Embedding-and-Hierarchical-Representation-to-Unlock-ADL-Rhythm-in-Smart-Homes/blob/master/Paper/Annexes.pdf>.

2 Related Works

2.1 Human Activity Recognition and Pre-trained Embeddings

Recent advances in deep learning have significantly impacted various fields, including HAR. In HAR, sensor-based deep learning techniques are pertinent to Convolutional Neural Networks [20, 15], autoencoders [23], semantics-based approaches [26], and sequence models [9]. Despite their efficacy, these methods often struggle with

* Email: damien.bouchabou@gmail.com

** Email: nguyensmai@gmail.com

temporal aspects, long-term dependencies, and pattern similarities crucial for recognizing ADLs.

In [12] Huang et Zhang have employed a transformer architecture [22] with handcrafted features to classify pre-segmented activities on the Aruba dataset from the CASAS benchmark [5]. However, their approach had limitations: it omitted the infrequent "respirate" activity and the "Other" category, which includes unidentified activities that share patterns with recognized ones. Additionally, their model had difficulty distinguishing similar activities like "wash dishes" and "meal preparation," and did not fully utilize deep learning's potential for automatic feature extraction.

Advancements in self-supervised learning and sequence modeling, such as bi-LSTM [13], ELMo [4], and GPT-2 [21], have influenced HAR. [4] enhanced bi-LSTM classifiers with a frozen, pre-trained ELMo-based sensor embedding. [21] used a GPT-2 architecture for predicting sensor events, but this approach was limited to feature engineering and did not leverage GPT-2's capabilities for classification tasks. Additionally, it lacked extensive analysis of embeddings, attention mechanisms, and ablation studies.

2.2 Hierarchical Models of Actions

A hierarchical approach is crucial for modeling human actions and recognizing ADLs in smart homes. Various hierarchical models have been developed using the CASAS dataset [5]. For example, [11] explored ontology models for context-aware activities, and [1] used Hierarchical Hidden Markov Models. These methods, however, have limitations in recognizing long-term dependencies.

Hierarchical LSTM models have also been applied to activity recognition with wearable sensors [24] and RGB-D videos [6]. [6] found that hierarchical structures improved recognition performance by processing more information from longer time windows and better understanding activity relationships, highlighting the importance of multi-level time dependencies.

ADLs, such as cooking or cleaning, can vary significantly daily based on the inhabitant's context and goals. Each activity comprises a sequence of unit actions, as identified in [6] and [24], organized to achieve a distant goal. Activities may also be interdependent, influencing and relying on each other.

3 Approach

3.1 Problem Formulation

Let $e_i = (i_i, v_i, t_i)$ be a sensor event, where $i_i \in \{1, \dots, n\}$ is the sensor ID, $v_i \in \mathcal{V}$ is the sensor value (binary or scalar), and $t_i \in \mathcal{T}$ is the timestamp. Events arrive asynchronously and form a history, or event stream. It is denoted as h_t , where t represents the current timestamp :

$$h_t = \langle e_1 = (i_1, v_1, t_1), e_2 = (i_2, v_2, t_2), \dots, e_k = (i_k, v_k, t_k) \rangle$$

where $\forall i \in \{1, \dots, k\}, t_i \leq t$

We note \mathcal{H} the set of histories supposed segmented into sensor event sequences, defined as a set of sensor events $s_j = \{e_1, \dots, e_L\}$. We note \mathcal{S} as the set of all sequences and $t_{s_j} = \max\{t_i, \text{ where } e_i = (i_i, v_i, t_i) \in s_j\}$ the timestamp of the last event of s_j .

Let $\mathcal{A} = \{a_1, \dots, a_m\}$ be the set of activity labels. The HAR problem learns to associate a sequence to a label given the history $f : \mathcal{S} \times \mathcal{H} \rightarrow \mathcal{A}$, where $f(s_j, h_{t_{s_j}}) \mapsto a_k$. Our approach decomposes f into three functions :

(1) Embedding $E_{\text{sequence}} : \{(i_1, v_1), \dots, (i_L, v_L)\} \rightarrow \mathbb{R}_{\text{sensor}}^d$

(2) Embedding $E_{\text{timestamp}} : \{t_1, \dots, t_L\} \rightarrow \mathbb{R}_{\text{time}}^d$

(3) Classification $C : (\mathbb{R}_{\text{sensor}}^d, \mathbb{R}_{\text{time}}^d)^c \rightarrow \mathcal{A}$, with c context length. Our implementation uses $c = 3$.

The hierarchical model is expressed as:

$$f(s_j, h_{t_{s_j}}) = C(E_{\text{sequence}}(s_{j-2}), E_{\text{timestamp}}(s_{j-2}), E_{\text{sequence}}(s_{j-1}), E_{\text{timestamp}}(s_{j-1}), E_{\text{sequence}}(s_j), E_{\text{timestamp}}(s_j))$$

where s_{j-2}, s_{j-1}, s_j are three consecutive event sequences. Dataset details are in Annex D.

3.2 Decoder Transformer Embedding

In the realm of HAR within smart homes, our approach builds upon the innovative application of pre-trained ELMo embeddings for ambient sensors, as proposed by [4], and the transformative successes of transformer architectures like BERT [7] and GPT [17]. We advance this field by adopting a Transformer decoder embedding architecture to enhance the performance of HAR algorithms.

Our primary goal is to improve HAR algorithms' ability to accurately categorize pre-segmented, temporally connected sequences of sensor events into identifiable daily activities. For instance, consider a scenario where a resident prepares to take a bath, involving a sequence of sensor-triggered events: leaving a room, going to the bathroom, opening the bathroom door, turning on the light, entering the bathroom, and using the shower. These activities imply a sequential relationship, where actions such as the bathroom door opening and entering the bathroom precede shower usage. This sequencing becomes critical in a multi-resident setting, where concurrent activities, like cooking, may occur. The model must distinguish related events from unrelated ones, focusing its attention to accurately extract the current activity context.

While ELMo and BERT excel in contextual understanding within sequences, their training approach limits their efficacy in addressing contexts beyond immediate sequences. They primarily capture context within pre-segmented sequences. In contrast, a Transformer decoder-based architecture like GPT, trained on data chunks that do not correspond to pre-segmented activity sequences, is more suitable for our needs as it learns longer-term dependencies and broader cause-and-effect relationships among sensor events.

Furthermore, the use of both past and future information in ELMo and BERT architectures to contextualize elements within a sequence prevents the reuse of these approaches for real-time ADL recognition. The Transformer decoder architecture, exemplified by GPT, addresses this limitation through its causal masking feature, which ensures that the network considers only previous sensor states to predict subsequent ones. This training approach enables the network to recognize and understand cause-and-effect relationships effectively.

As illustrated in Fig. 1, we integrate a pre-trained, frozen GPT Transformer decoder embedding as a replacement for the previous ELMo setup within our single-level temporal framework. This GPT embedding encodes sensor events E_{sequence} , which are subsequently processed by a Bi-LSTM layer, followed by a classification head with a Softmax layer C . This model forms the foundation of our classifier GPTAR.

3.3 Multi-Timescale Architecture

Motivated by the need to discern intricate temporal relationships both within individual activities and across successive ones, we designed a hierarchical architecture, as depicted in Fig. 2. Recognizing that human behaviors manifest across diverse observational scales, our

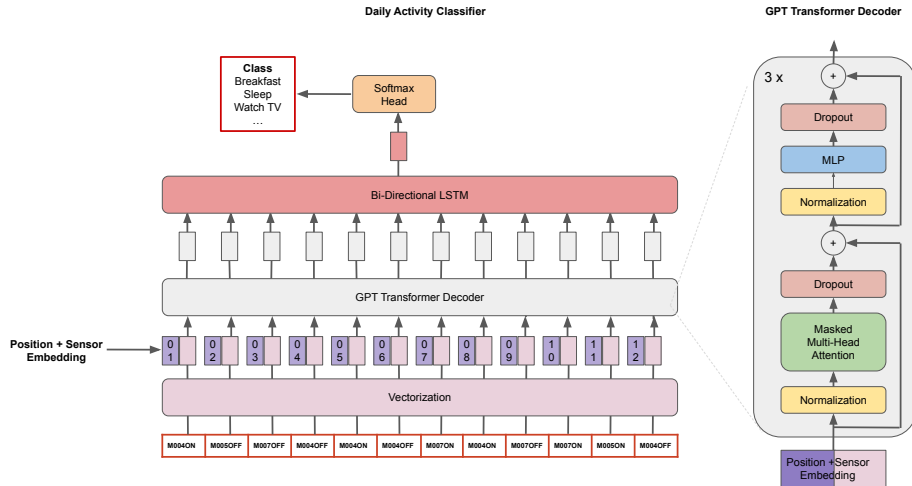


Figure 1: Model architecture of GPTAR and its GPT transformer decoder. GPTAR embeds the sensor signal with 3 layers of GPT transformer decoder embedding and a bi-LSTM. The illustration of the Transformer decoder was inspired by [22]

model comprehensively understands both the immediate sequences of events and the broader dynamics between activities.

We enhanced our architecture with an additional bi-directional LSTM layer, drawing methodological inspiration from the strategies proposed in [6]. This enhancement allows our model to not only discern immediate sequences of events but also to contextualize activities within a broader temporal framework. The bi-directionality of this LSTM layer enables it to capture insights from both prior and subsequent events, effectively integrating immediate event transitions with overarching behavioral patterns, thus providing a comprehensive understanding of human activity sequences.

For the input, our model processes a chronologically ordered sequence of three activities. This architectural choice is strategically made to predict the label of the current activity by leveraging the contextual representations of its two preceding activities. We opted for a sequence of three activities ($c = 3$) based on observations that activities often intersperse with a category termed "other," representing unlabeled sequences of sensor activations.

3.4 Time Encoding

In smart home human activity recognition, human behaviors often exhibit rhythmic patterns driven by ingrained habits. For example, sensor activation in the kitchen at 8 am might indicate breakfast, whereas the same trigger at 8 pm could relate to dinner.

We incorporate a specialized temporal encoding $E_{\text{timestamp}}$, as depicted in Fig. 2. A supplementary input maps to the hours corresponding to each sensor activation timestamp. For every sensor activation in the main input sequence, a corresponding hour-of-the-day value is aligned in this secondary time input sequence. These hour values are vectorized through an embedding layer, which are then processed by a bi-directional LSTM. The output from this LSTM combines with the output from the bi-directional LSTM that encodes the sensor activations, directed to a terminal LSTM layer designed to discern the intricate relationships and order of activities.

4 Methods

4.1 Datasets

To evaluate the robustness and adaptability of our model, we utilized from the CASAS collection [5] three datasets : Aruba to test

single-resident scenarios, Milan to assess the impact of pets and sensor issues, and Cairo to observe performance in multi-resident settings with overlapping activities. Collected from volunteers' homes over several months, these datasets feature unbalanced classes and vary in house structures and resident numbers¹.

4.2 Generative Pre-trained Transformer Sensor Embedding

Following the methodology outlined by [4], we employ a GPT transformer decoder [17] for training our sensor embedding. This model predicts the next sensor event based on the current context, employing natural language processing techniques to comprehend the logical sequence of human actions through sensor activations. As depicted in Figure 1, our GPT Sensor Embedding model includes token and positional embeddings, along with transformer decoders featuring pre-normalization [25], aligning with the GPT-2 [18] architecture. We utilized a context length of 1024 tokens for input contexts, consistent with the GPT-2 model's configuration.

4.3 Pre-processing, Training, Evaluation and Metrics

Datasets are divided weekly to preserve temporal relationships. Once partitioned, the weeks are shuffled and split into training (70%) and testing (30%) subsets. The training subset serves multiple purposes, including training of pre-trained embeddings, hyperparameter optimization through cross-validation, and training of the classifier.

During the embedding pre-training step, 80% of the training subset is used for model training, with the remaining 20% for validation. Early stopping, based on validation perplexity, is employed to prevent overfitting. For hyperparameter tuning, we utilize a 3-fold cross-validation method. From the first two folds, 20% is reserved for validation and early stopping, with the third fold serving as the test set for this phase. In the final classification stage, 20% of the whole training subset is earmarked for validation and early stopping, followed by testing on the initially defined test set.

Given the significant imbalance in our activity classes, we primarily report the F1-score metric to provide an unbiased estimate of performance. For statistical robustness, results are averaged over 10 repetitions, and all experiments are conducted with a fixed value for random seeds to ensure reproducibility.

¹ Additional details are provided in Annex D of the supplementary material

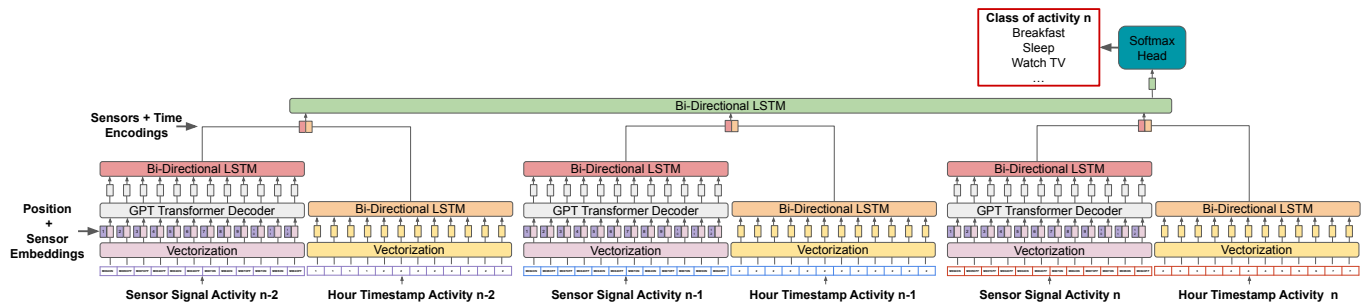


Figure 2: Complete architecture of the Generative Pre-trained Transformer for Hierarchical Activity Recognition (GPTHAR), composed of 3 low-level modules to compute 3 successive activities, and a top-level composed of a bi-LSTM and a softmax classifier. The low-level module processes in parallel the hour timestamp with a bi-LSTM and the sensor signal with a GPT transformer decoder embedding and a bi-LSTM

4.4 Vectorization of Sensor Activations

Sensor activations are categorized as distinct symbols, facilitating the model’s ability to identify patterns and relationships among activations, forming a comprehensive vocabulary of sensor actions. Our datasets include readings from motion (M), door (D), and temperature (T) sensors, each event logged with a unique sensor ID, corresponding value, and timestamp. Events are converted into unique tokens by merging sensor ID (i_i) and value (v_i), while the timestamp (t_i) is excluded. For example, a motion sensor M001 turning ON is tokenized as 'M001ON', and a temperature reading from sensor T004 at 24.5°C is represented as 'T00424.5'.

These tokens are indexed using natural language processing techniques, where indexing starts at 1, with 0 reserved for padding. The frequency of occurrence determines the index of each token, ensuring frequently appearing tokens are indexed with lower numbers. Thus, a sensor activation sequence like [M005OFF, M007OFF, M004OFF, M004ON] is transformed into an indexed sequence like [1, 4, 8, 2], reflecting the prevalence of each token.

5 Results

We address these research questions through empirical studies:

- RQ1 Can GPT-based embeddings better capture long-term dependencies and improve activity recognition accuracy?
- RQ2 Is a single-level long-term dependency model sufficient for modeling activities of daily living, and what additional benefits does a hierarchical model provide?
- RQ3 Is temporal information relevant for HAR, especially given the irregular sampling of time-series data from event-triggered sensors?

In this section we provide an empirical study of the following research questions: (RQ1) Can GPT-based models capture better long-term dependencies and lead to better activity recognition? (RQ2) Is a single-level long-term dependency enough to model activities of daily living and what does a hierarchical model add? (RQ3) Is time a relevant information for HAR, especially in the case of this irregularly sampled time-series from event-triggered sensors?

To investigate these questions, we conducted ablation studies with:

- GPTHAR, our proposed method, employs a GPT transformer decoder with time-encoding and a hierarchical architecture as depicted in Fig. 2.
- GPTHAR-note (no temporal encoding) uses a GPT transformer decoder in a hierarchical architecture (no timestamp information).
- GPTAR (see Fig. 1) uses a GPT transformer decoder as embedding in a single-level architecture (no timestamp information).

Table 1: Hierarchical Model: Test Mean F1-scores for FCN, Liciotti et al., and both hierarchical and non-hierarchical architectures using ELMo and GPT Embeddings. The ELMoAR and ELMoHAR models utilized a 60-token context window, while the GPTAR and GPTHAR model was configured with 8 attention heads and 3 layers.

	Aruba		Milan		Cairo	
	F1 Score	std	F1 Score	std	F1 Score	std
FCN [2]	33.10%	2.23	15.10	1.52	7.60%	2.46
Bi-LSTM [13]	32.00%	1.56	17.40%	2.07	26.60%	3.24
ELMoAR (W-size 60)	84.80%	1.99	70.80%	0.92	70.50%	1.43
GPTAR (8H 3L)	86.10%	1.20	70.80%	1.40	73.20%	1.99
ELMoHAR-note	88.10%	1.20	77.40	1.65	75.90%	2.88
GPTHAR-note	87.30%	2.98	79.90%	1.52	84.80%	1.81

- ELMoHAR, which uses ELMo as an embedding, combined with time-encoding and a hierarchical architecture.
- ELMoHAR-note (no temporal encoding) uses ELMo and a hierarchical architecture without timestamp information.
- ELMoAR, which applies ELMo for embedding in a single-level architecture without timestamp information.

5.1 Hyperparameters Search and Comparative Study

To address RQ1, we compared the embeddings: our GPT decoder Transformer-based model (GPTAR) and the ELMo-based model (ELMoAR) as described in [4]. Both models adhere to the architecture shown in Fig. 1, differing in the embedding. Each embedding was pre-trained using sensor activations, with the GPT decoder applied to unsegmented data and ELMo to pre-segmented data.

At first, we conducted hyperparameter tuning for each embedding technique, adjusting the context window size for ELMoAR and the number of layers and attention heads for GPTAR². The ELMoAR model, configured with a 60-token context window, provided the best results across datasets for ELMo-based models. For GPTAR, a configuration with 8 attention heads and 3 decoder layers yielded the best average F1 scores, especially in the noisier Milan and Cairo datasets.

Subsequently, using the selected embedding parameters, we conducted the final training and classification tasks for the ELMoAR and GPTAR architectures. In addition, we evaluated their performance against other methodological approaches: the Fully Convolutional Network (FCN), which has shown effective performance in time series classification [8] and ADL recognition [2], and a SOTA LSTM-based method known for its strong results in ADL recognition [13]³. The F1 scores are reported in Table 1⁴. The results demonstrate that

² The results of a 3-fold cross-validation on three datasets are reported in Table 7 in Annex A of the supplementary material

³ For details of the LSTM-based method, please refer to Annex E.

⁴ additional metrics and details are provided in Annex B of the supplementary material

both ELMoAR and GPTAR surpass the LSTM-based approach and the FCN in performance. Notably, while the LSTM method excels during training, it exhibits a significant drop in performance during testing. FCN struggles to effectively manage the length variability inherent in the sequences. In particular, the results indicate that GPTAR outperformed ELMoAR in the Aruba and Cairo datasets, although both models achieved the same F1 score on the Milan dataset.

Table 2: F1-Score by activity for each algorithm on the Aruba dataset

	ELMoAR	GPTAR	ELMoHAR-note	GPThAR-note	ELMoHAR	GPThAR
Bed_to_Toilet	0.987	0.996	0.991	0.992	0.992	0.996
Eating	0.925	0.935	0.937	0.948	0.932	0.936
Enter_Home	0.8	0.797	0.992	0.994	0.99	0.992
Housekeeping	0.83	0.84	0.829	0.907	0.852	0.918
Leave_Home	0.827	0.811	0.992	0.992	0.99	0.99
Meal_Preparation	0.974	0.971	0.972	0.968	0.971	0.964
Other	0.988	0.99	0.99	0.99	0.99	0.99
Relax	0.99	0.99	0.991	0.993	0.994	0.992
Respirate	0.867	0.967	0.651	0.502	0.967	0.548
Sleeping	0.988	0.99	0.982	0.984	0.991	0.981
Wash_Dishes	0.008	0.047	0.266	0.243	0.225	0.199
Work	0.984	0.993	0.979	0.987	0.985	0.975

Table 3: F1-Score by activity for each algorithm on Milan dataset

	ELMoAR	GPTAR	ELMoHAR-note	GPThAR-note	ELMoHAR	GPThAR
Bed_to_Toilet	0.551	0.532	0.79	0.749	0.845	0.902
Chores	0	0.011	0.088	0.122	0.15	0.161
Desk_Activity	0.976	0.996	0.952	0.982	0.958	0.976
Dining_Rm_Activity	0.416	0.252	0.516	0.481	0.491	0.522
Eve_Meds	0	0.095	0.421	0.587	0.566	0.545
Guest_Bathroom	0.978	0.981	0.979	0.98	0.98	0.984
Kitchen_Activity	0.91	0.919	0.93	0.936	0.927	0.931
Leave_Home	0.901	0.911	0.934	0.952	0.941	0.957
Master_Bathroom	0.884	0.858	0.942	0.943	0.968	0.977
Master_Bedroom_Activity	0.788	0.792	0.799	0.836	0.836	0.872
Meditate	0.86	0.874	0.863	0.933	0.866	0.972
Morning_Meds	0.58	0.546	0.642	0.669	0.698	0.712
Other	0.888	0.9	0.906	0.92	0.909	0.924
Read	0.92	0.946	0.917	0.947	0.914	0.953
Sleep	0.897	0.921	0.927	0.925	0.943	0.932
Watch_TV	0.767	0.778	0.782	0.807	0.789	0.806

Table 4: F1-Score by activity for each algorithm on Cairo dataset

	ELMoAR	GPTAR	ELMoHAR-note	GPThAR-note	ELMoHAR	GPThAR
Bed_to_toilet	0.382	0.359	0.374	0.483	0.545	0.311
Breakfast	0.533	0.61	0.822	0.89	0.886	0.94
Dinner	0.415	0.412	0.711	0.713	0.961	0.991
Laundry	0.911	1	0.309	0.951	0.358	0.794
Leave_home	0.938	0.958	0.891	0.97	0.895	0.973
Lunch	0.337	0.331	0.609	0.67	0.912	0.929
Night_wandering	0.759	0.795	0.805	0.829	0.823	0.837
Other	0.915	0.923	0.948	0.968	0.955	0.977
R1_sleep	0.702	0.629	0.852	0.868	0.897	0.877
R1_wake	0.871	0.899	0.903	0.906	0.895	0.909
R1_work_in_office	0.853	0.939	0.918	0.985	0.92	0.991
R2_sleep	0.706	0.715	0.824	0.857	0.856	0.863
R2_fake_medicine	0.781	0.913	0.859	0.94	0.87	0.931
R2_wake	0.745	0.746	0.799	0.821	0.852	0.87

However, an analysis of individual activity performance with F1-scores per activity in Tables 2, 3 & 4 and the confusion matrices in Fig.3 & 4 revealed specific challenges⁵. Activities such as ‘Wash Dishes’ in Aruba, ‘Eve Meds’ in Milan, and ‘Laundry’ in Cairo showed better recognition by GPTAR. These activities exhibit similar sensor patterns to other activities, such as between ‘Meal Preparation’ and ‘Wash Dishes’ in Aruba. ‘Eve Meds’ ’s confusion with ‘Kitchen Activity’ by ELMo (see green dots top right corner) is partially resolved by GPT. Fig. 5 shows that the ‘Laundry’ data in Cairo are embedded closer together by GPT than ELMo.

5.2 Hierarchical Activity Recognition

To investigate RQ2, we compare GPTAR and ELMoAR with the hierarchical models versions without time encoding, GPThAR-note and ELMoHAR-note respectively. These models omit the timestamp inputs depicted in Fig. 2. Our analysis in Sections 5.2.1 and 5.2.2 evaluates whether hierarchical models, which aim to capture complex inter-activity relationships, outperform non-hierarchical models that utilize longer input contexts and activity segmentation markers.

⁵ see all confusion matrices in Annex C

5.2.1 Comparison of Hierarchical Architectures

As with previous experiments, the pre-trained embeddings were maintained frozen, with only the dual bi-directional LSTM layers and the softmax layer undergoing further training for classification.

Table 1 illustrates that the hierarchical structure effectively leverages both types of pre-trained embeddings to enhance performance. While GPThAR-note shows substantial improvements over ELMoHAR-note in the Milan and especially Cairo datasets, it slightly lags behind in the Aruba dataset, suggesting that GPThAR-note performs better in more complex, noisy environments. However, employing a hierarchical structure has led to increased standard deviation, indicating a reduction in performance consistency. We hypothesize that a regularization layer following the embedding output could stabilize the model’s performance.

Comparison of GPThAR-note to GPTAR, and ELMoHAR-note to ELMoAR for each activity F1 scores in Tables 2, 3 & 4 and confusion matrices⁶ in Fig. 3 & 4 reveals that sequential activities such as, in Milan, ‘Dining Room Activity’, ‘Meditate’ and ‘Watch TV’ are less confused with ‘Other’ activity; and ‘Eve Med’, ‘Morning Meds’ are less confused with ‘Kitchen activity’. Moreover, in Cairo, ‘Dinner’, ‘Breakfast’ and ‘Lunch’ are less confused by the hierarchical models.

5.2.2 Input Context Extended

To assess the efficacy of the hierarchical structure, we conducted a comparative analysis between hierarchical and non-hierarchical model configurations using an augmented input context. Specifically, we extended the input for the base models, ELMoAR and GPTAR, by: 1) appending two preceding activities to the current one, while maintaining temporal sequences order, and 2) incorporating two preceding activities with a separation token, < SEP > delineating distinct sensor sequences. This token is designed to clearly mark activity boundaries, a task inherently managed by the hierarchical models.

The F1-scores presented in Table 5, confirm that hierarchical models consistently outperform their non-hierarchical counterparts with extended input contexts. Despite the addition of a separation token to non-hierarchical models to indicate sequence segmentation, leading to some improvements in F1-score, yet, hierarchical structures still demonstrated superior performance across all three datasets.

Furthermore, our observations revealed that increasing the number of nodes in the last bi-directional LSTM layer of the non-hierarchical models improved performance for both the extended context and the extended context with separator setups. However, these enhancements were still insufficient to match the performance levels achieved by the hierarchical structures.

5.3 The Impact of Time Encoding

To address RQ3, we compare models with and without this time encoding (ELMoHAR and GPThAR with encoding; ELMoHAR-note and GPThAR-note without) in Table 6⁷.

The integration of the temporal component significantly enhances the classification efficacy of both models, notably by reducing the standard deviation. In the Milan and Cairo datasets, GPThAR substantially outperforms ELMoHAR and ELMoHAR-note. An examination of the confusion matrices⁸ in Fig. 4 reveals that in the Cairo dataset, activities like ‘Laundry’ are better recognised. In the Aruba

⁶ see complete results in Annex C

⁷ additional metrics in Annex B

⁸ see all in Annex C in the supplementary material

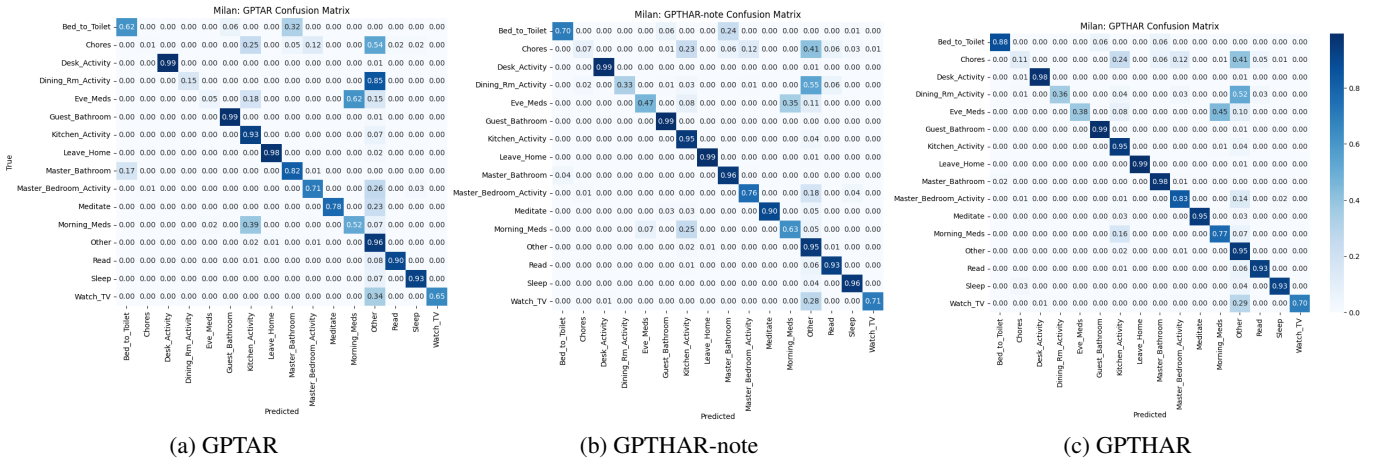


Figure 3: Confusion matrices per algorithm on the Milan dataset

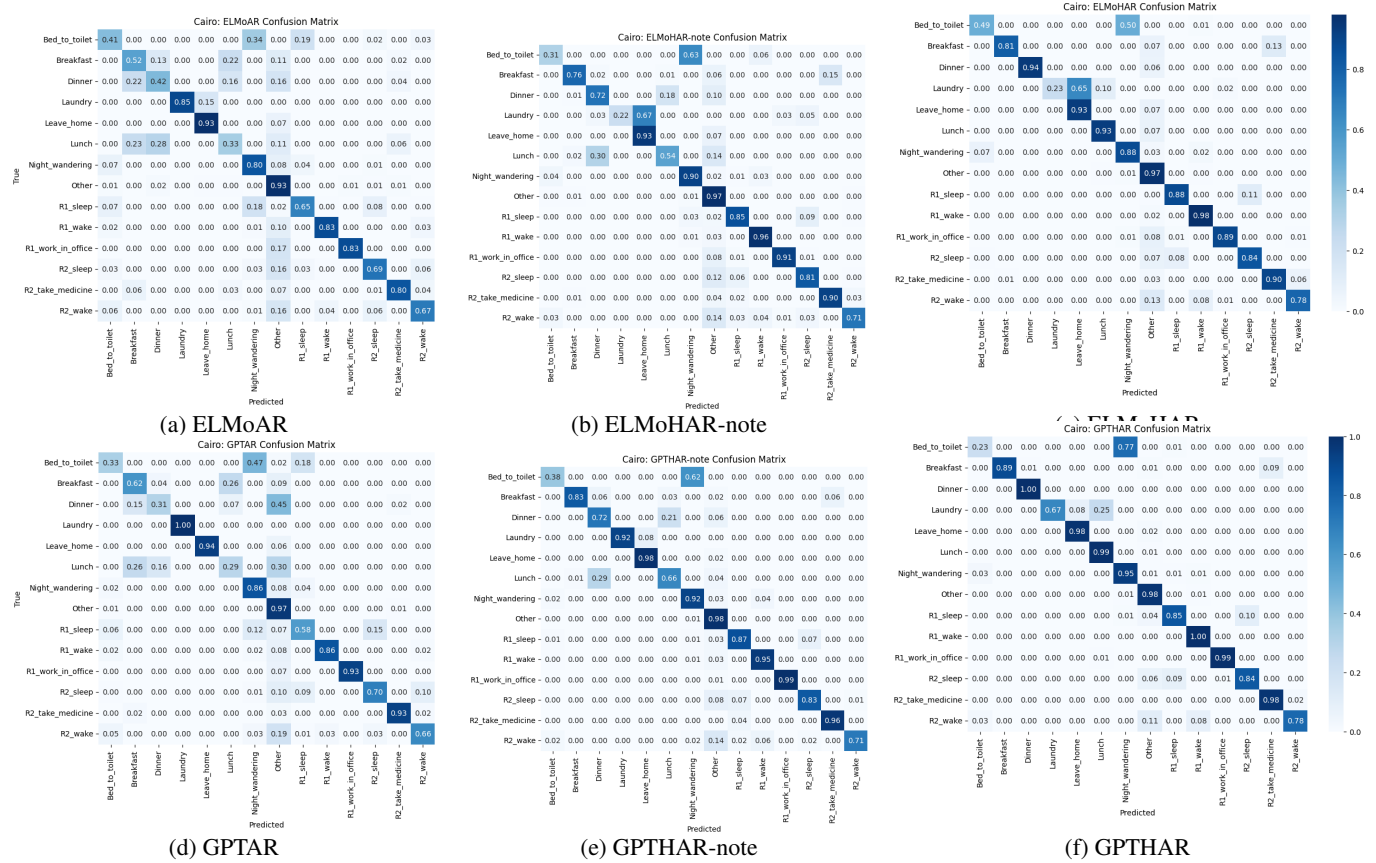


Figure 4: Confusion matrices per algorithm on the Cairo dataset

dataset, activities such as ‘Washing Dishes’, ‘Meal Preparation’, ‘Enter Home’, and ‘Leave Home’ exhibit improved classification accuracy. In Fig. 3 for Milan, activities like ‘Eve Med’ and ‘Morning Meds’ show a reduction in misclassifications.

5.4 Attention Heads through a Case Study

This case study examines the efficacy of GPT-based models and the role of its causal model. Fig. 4 previously showed that the recog-

nition of the ‘Laundry’ activity within the Cairo dataset improved both in GPTHAR (vs ELMoHAR) and in GPTAR (vs ELMoAR). are often erroneously identified as ‘Leave Home’ in models employing pre-trained ELMO embeddings (ELMoAR, ELMoHAR-note, and ELMoHAR). Indeed, Fig. 14 shows that an embedding of Laundry is very close to embeddings of Leave Home.

The dual-resident setting of the Cairo dataset exacerbates the issue of concurrent activities. Fig. 6 plots for a recording of ‘Laundry’ the activation sequence and attention heads by the GPT embedding,

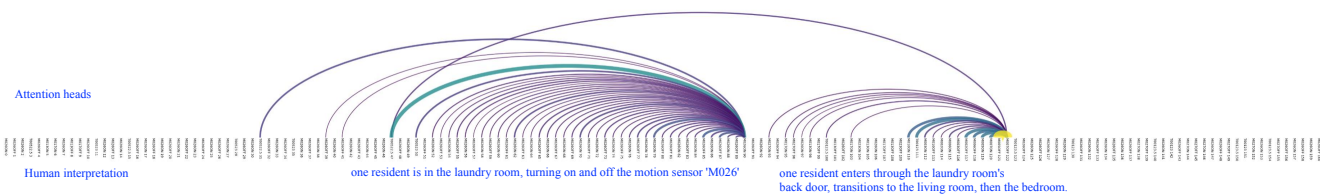


Figure 6: Visualization for GPT Transformer decoder on a "Laundry" sequence, of the attention heads leading to tokens 90 (M026ON) and 122 (M007OFF). The yellow and wide arcs indicate high attention; the blue and narrow arcs, a low attention. Time is read from left to right.

- [6] M. Devanne, P. Papadakis, and S. M. Nguyen. Recognition of activities of daily living via hierarchical long-short term memory networks. In *2019 IEEE International Conference on Systems, Man and Cybernetics (SMC)*, pages 3318–3324. IEEE, 2019.
- [7] J. Devlin, M.-W. Chang, K. Lee, and K. Toutanova. Bert: Pre-training of deep bidirectional transformers for language understanding. *arXiv preprint:1810.04805*, 2018.
- [8] H. I. Fawaz, G. Forestier, J. Weber, L. Idoumghar, and P.-A. Muller. Deep learning for time series classification: a review. *Data Mining and Knowledge Discovery*, 33(4):917–963, 2019.
- [9] A. Ghods and D. J. Cook. Activity2vec: Learning adl embeddings from sensor data with a sequence-to-sequence model. *arXiv preprint arXiv:1907.05597*, 2019.
- [10] M. Gochoo, T.-H. Tan, S.-H. Liu, F.-R. Jean, F. S. Alnajjar, and S.-C. Huang. Unobtrusive activity recognition of elderly people living alone using anonymous binary sensors and dcnn. *IEEE journal of biomedical and health informatics*, 23(2):693–702, 2018.
- [11] X. Hong, C. Nugent, M. Mulvenna, S. McClean, B. Scotney, and S. Devlin. Evidential fusion of sensor data for activity recognition in smart homes. *Pervasive and Mobile Computing*, 5(3):236 – 252, 2009. doi: <https://doi.org/10.1016/j.pmcj.2008.05.002>.
- [12] X. Huang and S. Zhang. Human activity recognition based on transformer in smart home. In *Proceedings of the 2023 2nd Asia Conference on Algorithms, Computing and Machine Learning*, pages 520–525, 2023.
- [13] D. Liciotti, M. Bernardini, L. Romeo, and E. Frontoni. A sequential deep learning application for recognising human activities in smart homes. *Neurocomputing*, 04 2019. doi: 10.1016/j.neucom.2018.10.104.
- [14] J. Medina-Quero, S. Zhang, C. Nugent, and M. Espinilla. Ensemble classifier of long short-term memory with fuzzy temporal windows on binary sensors for activity recognition. *Expert Systems with Applications*, 114:441–453, 2018.
- [15] G. Mohamed, A. Lotfi, and A. Pourabdollah. Employing a deep convolutional neural network for human activity recognition based on binary ambient sensor data. In *Proceedings of the 13th ACM International Conference on Pervasive Technologies Related to Assistive Environments*, pages 1–7, 2020.
- [16] M. E. Peters, M. Neumann, M. Iyyer, M. Gardner, C. Clark, K. Lee, and L. Zettlemoyer. Deep contextualized word representations. *arXiv preprint arXiv:1802.05365*, 2018.
- [17] A. Radford, K. Narasimhan, T. Salimans, I. Sutskever, et al. Improving language understanding by generative pre-training. 2018.
- [18] A. Radford, J. Wu, R. Child, D. Luan, D. Amodei, I. Sutskever, et al. Language models are unsupervised multitask learners. *OpenAI blog*, 1 (8):9, 2019.
- [19] M. Sedky, C. Howard, T. Alshammari, and N. Alshammari. Evaluating machine learning techniques for activity classification in smart home environments. *International Journal of Information Systems and Computer Sciences*, 12(2):48–54, 2018.
- [20] D. Singh, E. Merdivan, S. Hanke, J. Kropf, M. Geist, and A. Holzinger. Convolutional and recurrent neural networks for activity recognition in smart environment. In *Towards integrative machine learning and knowledge extraction*, pages 194–205. Springer, 2017.
- [21] N. Takeda, R. Legaspi, Y. Nishimura, K. Ikeda, A. Minamikawa, T. Plötz, and S. Chernova. Sensor event sequence prediction for proactive smart home support using autoregressive language model. In *2023 19th International Conference on Intelligent Environments (IE)*, pages 1–8, 2023. doi: 10.1109/IE57519.2023.10179111.
- [22] A. Vaswani, N. Shazeer, N. Parmar, J. Uszkoreit, L. Jones, A. N. Gomez, L. Kaiser, and I. Polosukhin. Attention is all you need. In *Advances in neural information processing systems*, pages 5998–6008, 2017.
- [23] A. Wang, G. Chen, C. Shang, M. Zhang, and L. Liu. Human activity recognition in a smart home environment with stacked denoising autoencoders. In *International conference on web-age information management*, pages 29–40. Springer, 2016.
- [24] L. Wang and R. Liu. Human activity recognition based on wearable sensor using hierarchical deep lstm networks. *Circuits, Systems, and Signal Processing*, 39(2):837–856, 2020. doi: 10.1007/s00034-019-01116-y.
- [25] R. Xiong, Y. Yang, D. He, K. Zheng, S. Zheng, C. Xing, H. Zhang, Y. Lan, L. Wang, and T. Liu. On layer normalization in the transformer architecture. In *International Conference on Machine Learning*, pages 10524–10533. PMLR, 2020.
- [26] N. Yamada, K. Sakamoto, G. Kunito, Y. Isoda, K. Yamazaki, and S. Tanaka. Applying ontology and probabilistic model to human activity recognition from surrounding things. *IPSSJ Digital Courier*, 3: 506–517, 2007.

A Hyper parameter search

In this appendix, we present F1 scores during cross-validation of ELMoAR and GPTAR with, respectively, different window sizes and different head and layer numbers. The best hyperparameters are selected for the ELMoHAR-note, ELMoHAR and GPTAR-note and GPTAR algorithms.

For ELMoAR, the best hyperparameters are: a window size of 60. For GPTAR, the best hyperparameters are : 8 attention heads and 3 layers of decoder.

Table 7: Cross-validation F1-Scores with their standard deviation for GPTAR and ELMoAR models with various hyperparameters across the three datasets, to assess the Impact of context window size in ELMoAR and the number of layers and attention heads in GPTAR

	Aruba		Milan		Cairo		Average
	Macro F1 Score	std	Macro F1 Score	std	Macro F1 Score	std	
ELMoAR (Window 20)	83.47	1.83	71.10	2.25	66.37	3.24	73.65
ELMoAR (Window 40)	82.93	2.12	70.73	2.43	66.70	4.07	73.45
ELMoAR (Window 60)	83.47	2.61	72.40	2.49	67.23	4.70	74.37
GPTAR (8 Heads 3 Layers)	83.20	1.45	73.77	2.19	70.90	3.48	75.96
GPTAR (8 Heads 4 Layers)	83.53	1.48	72.30	1.62	69.03	4.42	74.95
GPTAR (12 Heads 6 Layers)	83.57	1.57	73.07	2.13	68.27	4.08	74.97

B Detailed Algorithms Metrics

In this appendix, we present a comprehensive breakdown of the performance metrics for the algorithms used in our study. The table encompasses test results from three distinct datasets: Aruba (Table 8), Milan (Table 9), and Cairo (Table 10). These metrics show that for the most simple dataset, Aruba, ELMoHAR and GPTAR perform closely, ranking first or second depending on the chosen metric. For the more complex datasets, Milan and Cairo, GPTAR outperforms all the other algorithms, regardless of the choice of metric.

Table 8: Detailed Algorithms Scores over the datasets Aruba

	ELMoAR	GPTAR	ELMoHAR-note	GPTAR-note	ELMoHAR	GPTAR
Accuracy	97.00%	97.10%	98.40%	98.20%	98.50%	98.52%
Precision	86.00%	90.30%	89.90%	87.40%	94.30%	91.20%
Recall	84.70%	85.10%	88.10%	88.60%	89.70%	89.80%
F1 Score	84.80%	86.10%	88.10%	87.30%	90.70%	89.70%
Balanced Accuracy	84.76%	85.18%	88.22%	88.55	89.71%	90.10%
Weighted Precision	96.70%	97.00%	98.10%	98.00%	98.50%	98.00%
Weighted Recall	97.00%	97.00%	98.40%	92.20%	98.50%	98.30%
Weighted F1 Score	96.9%	97.00%	98.00%	98.00%	98.30%	98.20%

Table 9: Detailed Algorithms Scores over the dataset Milan

	ELMoAR	GPTAR	ELMoHAR-note	GPTAR-note	ELMoHAR	GPTAR
Accuracy	87.50%	88.20%	90.00%	91.30%	90.60%	91.9%
Precision	75.90%	80.20%	85.60%	87.60%	88.90%	90.00%
Recall	68.40	68.50%	73.90	76.90%	75.60%	79.20%
F1 Score	70.80%	70.80%	77.40%	79.90%	80.00%	81.90%
Balanced Accuracy	68.51%	68.55%	73.91%	76.87%	77.84%	79.22%
Weighted Precision	86.80%	88.20%	89.60%	91.20%	90.70%	91.90%
Weighted Recall	87.50%	88.20%	90.00%	91.30%	90.60%	91.90%
Weighted F1 Score	86.70%	87.60%	89.20%	90.70%	90.00%	91.70%

Table 10: Detailed Algorithms Scores over the dataset Cairo

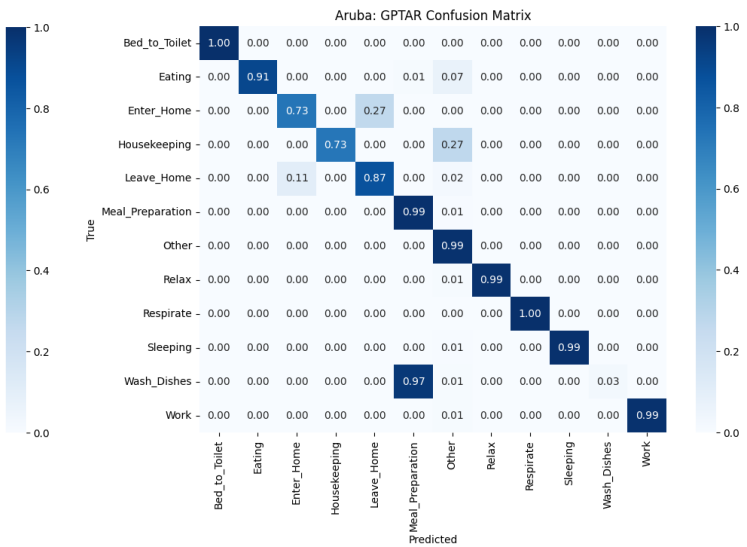
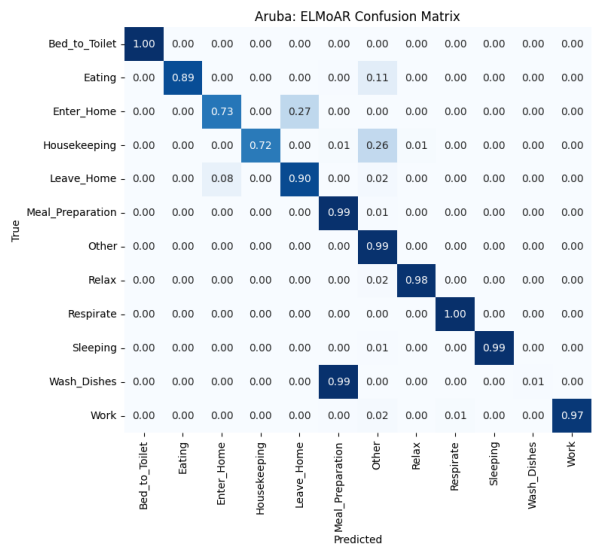
	ELMoAR	GPTAR	ELMoHAR-note	GPTAR-note	ELMoHAR	GPTAR
Accuracy	81.1%	83.40%	87.30%	91.00%	90.80%	93.20
Precision	72.70%	76.60%	79.70%	87.40%	87.30%	89.80%
Recall	69.20%	71.40%	74.70%	83.40%	82.00%	86.60%
F1 Score	70.50%	73.20%	75.90%	84.80%	83.30%	87.20%
Balanced Accuracy	69.12%	71.33%	74.75%	83.58%	81.87%	86.74%
Weighted Precision	81.10%	82.40%	86.90%	91.10%	90.60%	93.20
Weighted Recall	81.10%	83.40%	87.30%	91.00%	90.80%	93.20
Weighted F1 Score	80.90%	82.30%	86.80%	90.50%	90.30%	92.70%

C Confusion Matrix

In this section, we report on the confusion matrices for various algorithms across three datasets. A notable observation is that the more complex architectures, which include time encodings (namely ELMoHAR and GPTAR), exhibit fewer misclassifications compared to simpler models.

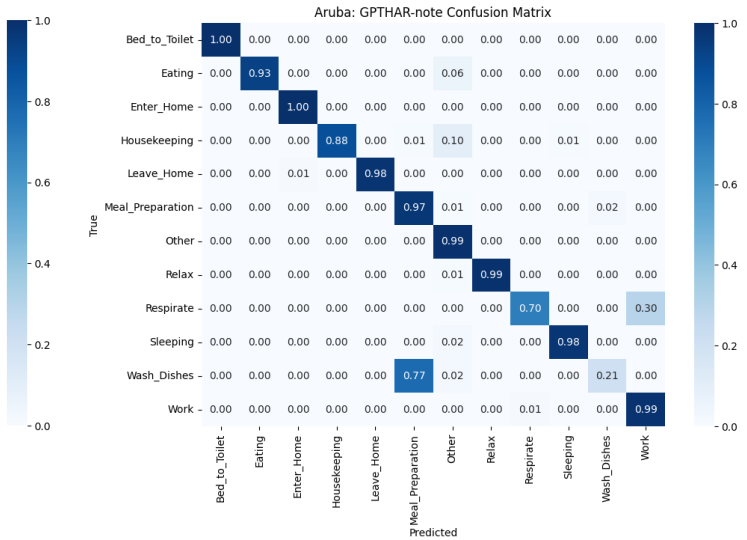
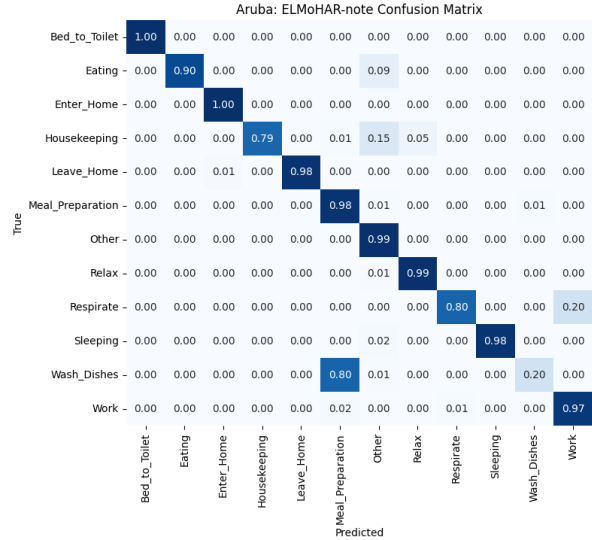
This improvement is particularly evident in specific activities. For instance, in the Aruba dataset, activities like 'Washing Dishes', 'Meal Preparation', 'Enter Home', and 'Leave Home' are classified more accurately. Similarly, in the Milan dataset, activities such as 'Eve Med' and 'Morning Meds' show a marked decrease in misclassifications. Additionally, in the Cairo dataset, meal-related activities like 'Breakfast', 'Lunch', and 'Dinner' are more accurately identified.

These findings highlight the effectiveness of our improved algorithms in reducing misclassifications.



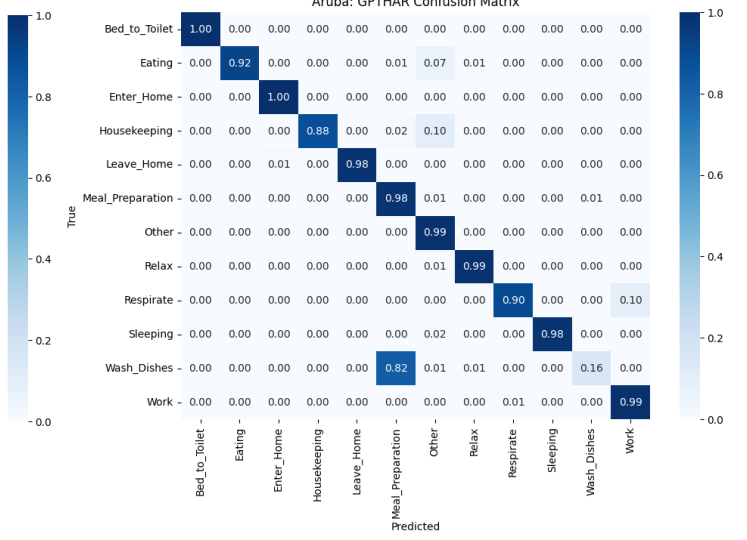
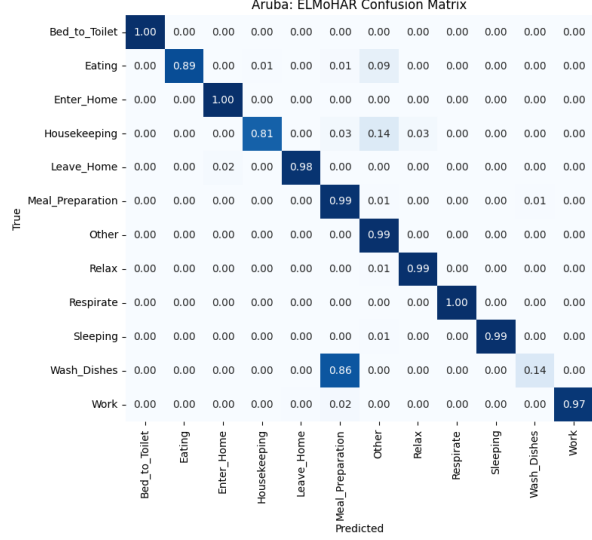
(a) ELMoAR

(b) GPTAR



(c) ELMoHAR-note

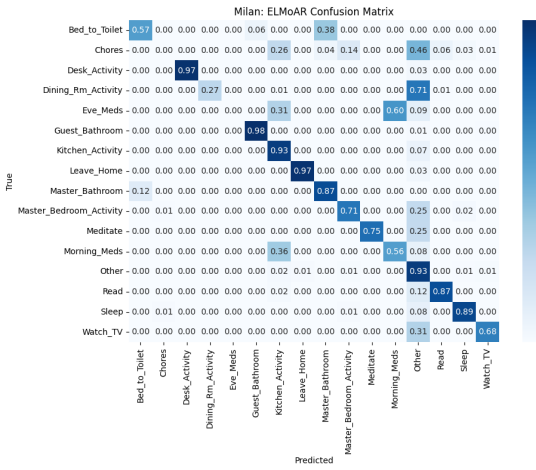
(d) GPTHAR-note



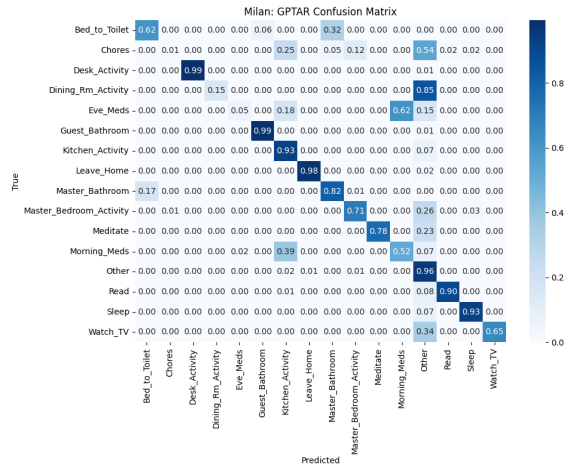
(e) ELMoHAR

(f) GPTHAR

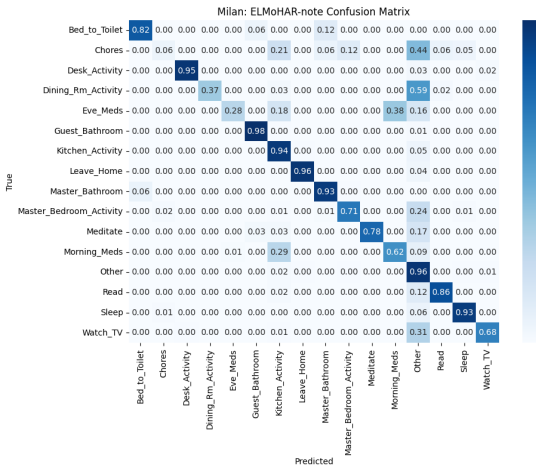
Figure 7: Confusion matrices per algorithm on the Aruba dataset.



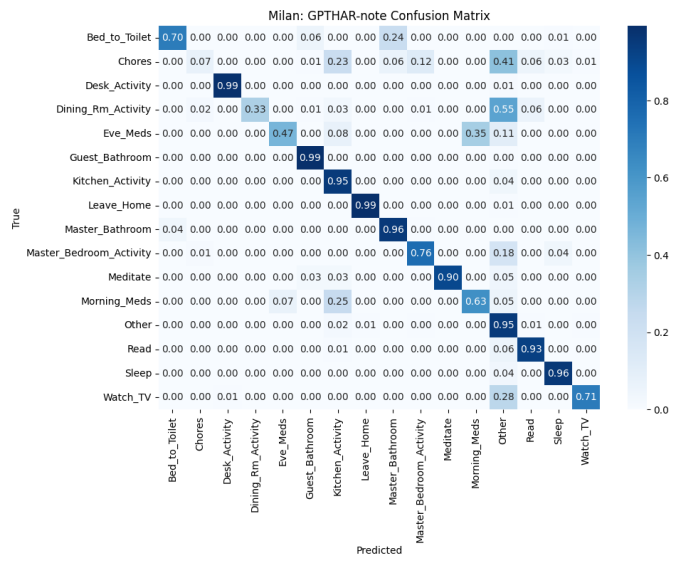
(a) ELMoAR



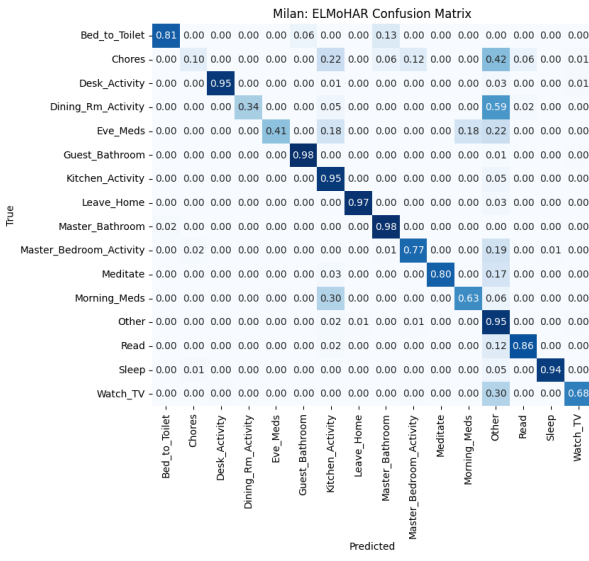
(b) GPTAR

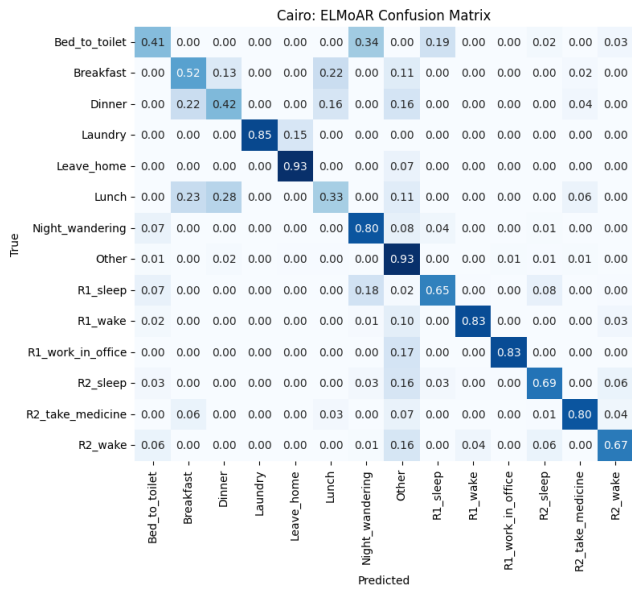


(c) ELMoHAR-note

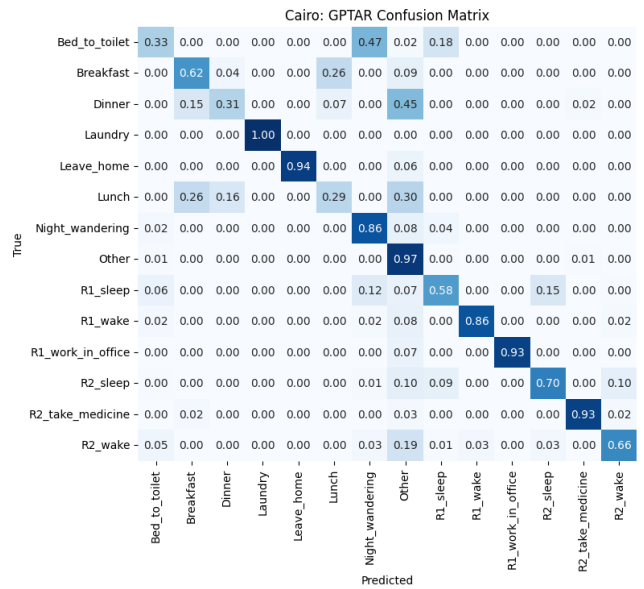


(d) GPTHAR-note

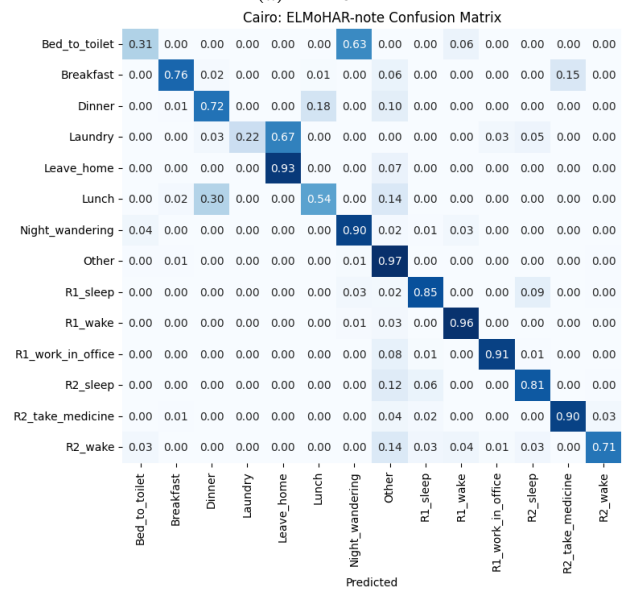




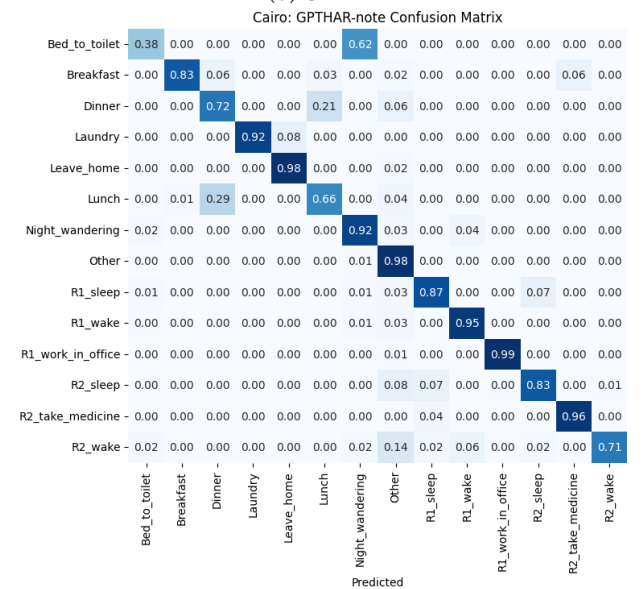
(a) ELMoAR



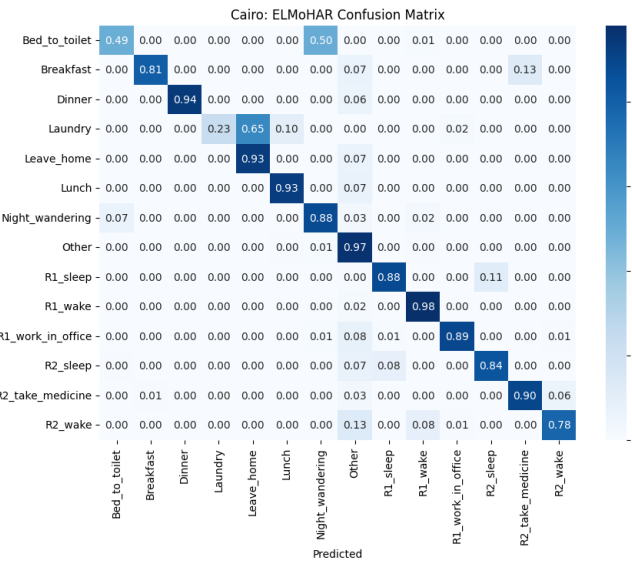
(b) GPTAR



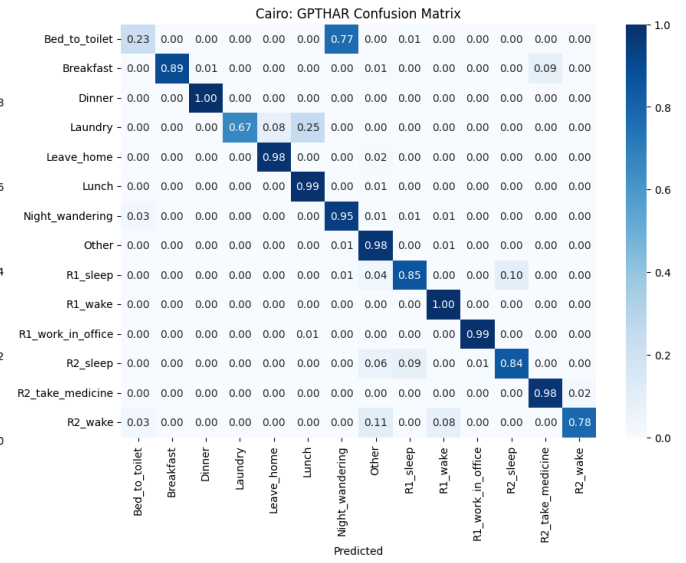
(c) ELMoHAR-note



(d) GPTHAR-note



(e) ELMoHAR



D Datasets Details

This appendix details information on three CASAS datasets—Aruba, Milan, and Cairo—created by Washington State University [5]. Data were collected from real homes equipped with smart sensors and inhabited by real residents. The sensor events log, as shown in Figure 10, comprises motion sensors (sensor IDs beginning with "M"), door closure sensors (sensor IDs beginning with "D"), and temperature sensors (sensor IDs beginning with "T"). Each log entry consists of a single event per row and includes six columns: date, timestamp, sensor ID, sensor value, activity during which the sensor was triggered, and the activity status (its beginning or its end). The datasets differ in housing structure, number of inhabitants, and the duration of activity labeling, with several months of data for each (details provided in Table 11). Floor maps for each dataset are illustrated in Figure 11.

Aruba and Milan feature single-floor homes with the same number of rooms but different layouts, whereas the Cairo home spans three floors and contains more rooms than the former two. The Aruba dataset captures the daily activities of a woman living alone, Milan documents the life of a woman and her dog, and Cairo describes a couple living with a dog.

The three datasets are unbalanced, with some activities less represented than others, as depicted in Table 12. This imbalance is due to the real-life settings of these homes and the lifestyles of the inhabitants. Furthermore the datasets do not cover exactly the same activities

10-11-04	05:40:51.303739	M004	ON	Bed_to_Toilet	begir
10-11-04	05:40:52.342105	M005	OFF		
10-11-04	05:40:57.176409	M007	OFF		
10-11-04	05:40:57.941486	M004	OFF		
10-11-04	05:43:24.021475	M004	ON		
10-11-04	05:43:26.273181	M004	OFF		
10-11-04	05:43:26.345503	M007	ON		
10-11-04	05:43:26.793102	M004	ON		
10-11-04	05:43:27.195347	M007	OFF		
10-11-04	05:43:27.787437	M007	ON		
10-11-04	05:43:29.711796	M005	ON		
10-11-04	05:43:30.279021	M004	OFF	Bed_to_Toilet	end
10-11-04	05:43:45.7324	M003	ON	Sleeping	begir
10-11-04	05:43:52.044085	M003	OFF		
10-11-04	05:43:53.185335	M002	ON		
10-11-04	05:43:53.253809	M003	ON		
10-11-04	05:43:59.493281	M002	OFF		

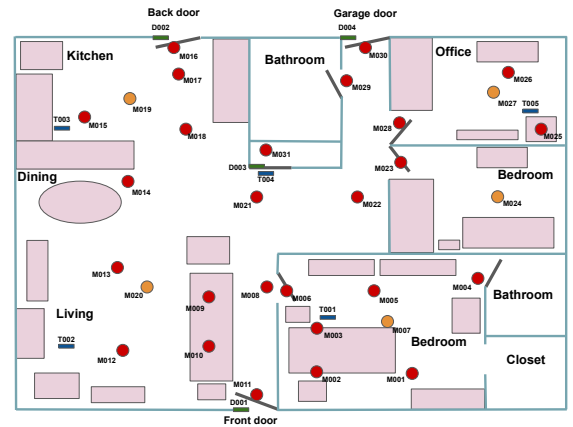
Figure 10: Extract of a CASAS dataset log

Table 11: Details of the three CASAS datasets

Dataset	Aruba	Milan	Cairo
Residents	1	1 + pet	2 + pet
Number of Sensors	39	33	27
Number of Activities	12	16	13
Number of Days	219	82	56

Table 12: Aruba, Milan and Cairo labels details.

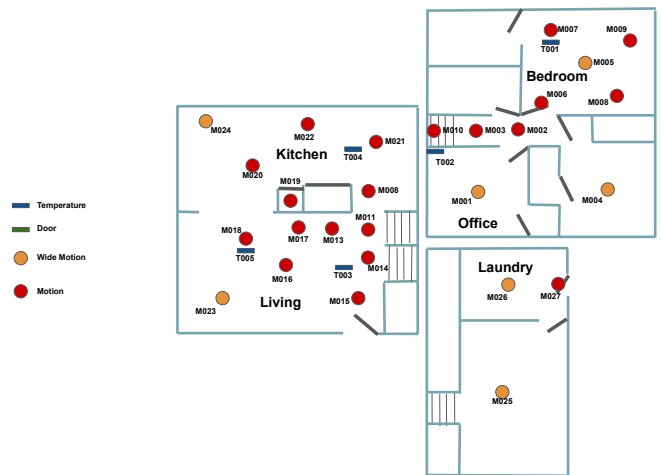
Aruba		Milan		Cairo	
Labels	# occurrence	Labels	# occurrence	Labels	# occurrence
Bed_to_Toilet	155	Bed_to_Toilet	86	Bed_to_toilet	29
Eating	262	Chores	32	Breakfast	49
Enter_Home	427	Desk_Activity	54	Dinner	42
Housekeeping	34	Dining_Rm_Activity	26	Laundry	10
Leave_Home	427	Eve_Meds	19	Leave_home	69
Meal_Preparation	1610	Guest_Bathroom	335	Lunch	37
Other	6079	Kitchen_Activity	741	Night_wandering	66
Relax	2944	Leave_Home	211	Other	579
Respirate	6	Master_Bathroom	307	R1_sleep	55
Sleeping	416	Master_Bedroom_Activity	204	R1_wake	53
Wash_Dishes	64	Meditate	17	R1_work_in_office	46
Work	171	Morning_Meds	41	R2_sleep	53
		Other	1776	R2_take_medicine	44
		Read	368	R2_wake	64
		Sleep	166		
		Watch_TV	153		



(a) Aruba dataset floor map



(b) Milan dataset floor map



(c) Cairo dataset floor map

Figure 11: Floor maps of Aruba, Milan, and Cairo Datasets.

E Experiments Reproduction

This appendix presents the scores and results of our replication of the Liciotti et al. [13] experiments. Table 13 below includes results from the original paper for the Milan and Cairo datasets, alongside our findings. It's important to note that the Aruba dataset was not explored in the original study. We conducted our experiments 10 times, and the table reflects the average results of these repetitions. In line with the original paper, we employed a 3-fold cross-validation evaluation method for each dataset and regrouping the original dataset labels under meta-activities using the same activity remapping as in the original study. Additionally, we adhered to the same hyperparameters defined in the original paper to ensure consistency in our replication process. Our findings demonstrate that we achieved results closely similar to those in the original paper, confirming the accuracy of our implementation of the algorithm.

Table 13: Reproduction results of the Bi-LSTM architecture as proposed by Liciotti et al. Our replication of these experiments was conducted 10 times to ensure reliability and consistency of the results.

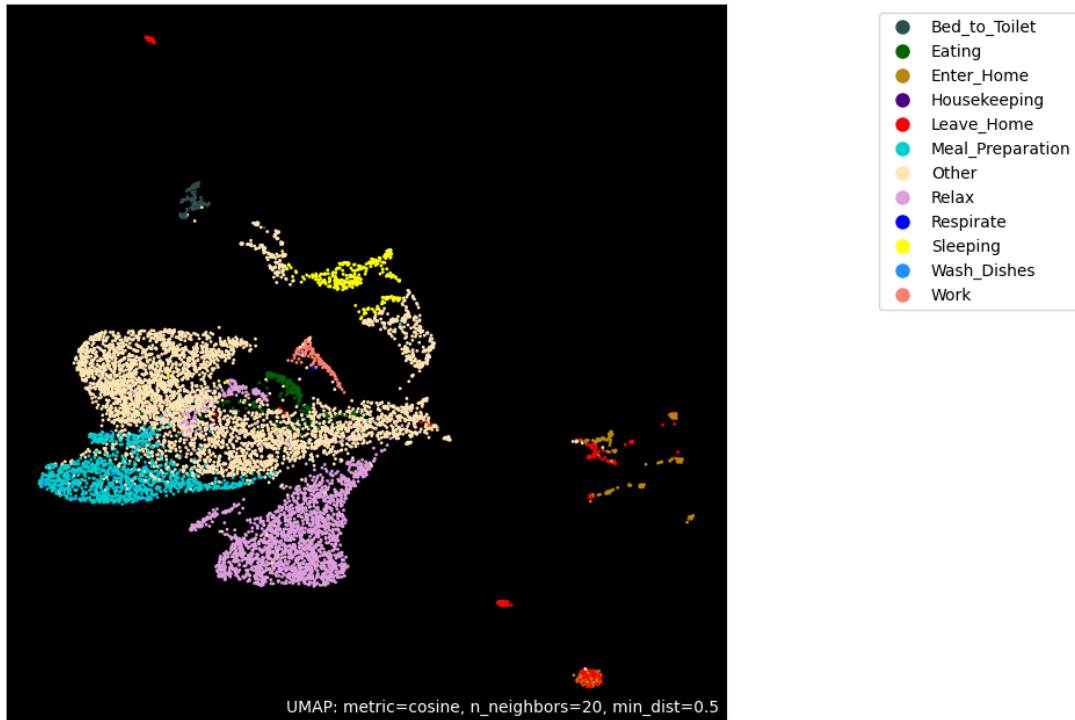
	Aruba		Milan		Cairo	
	Liciotti et al. (paper)	Liciotti et al. (reproduce)	Liciotti et al. (paper)	Liciotti et al. (reproduce)	Liciotti et al. (paper)	Liciotti et al. (reproduce)
Accuracy	NA	96.17%	94.12%	90.70%	86.90%	86.67%
Precision	NA	92.73%	NA	82.33%	NA	79.67%
Recall	NA	90.17%	NA	77.00%	NA	75.00%
F1 Score	NA	91.17%	NA	79.33%	NA	76.33%
Balanced Accuracy	NA	90.37%	NA	76.88%	NA	74.98%
Weighted Precision	NA	96.30%	94.00%	90.33%	86.67%	86.33%
Weighted Recall	NA	96.10%	94.00%	90.67%	87.00%	86.67%
Weighted F1 Score	NA	96.03%	94.00%	90.33%	86.67%	86.33%

F Activities Embedding

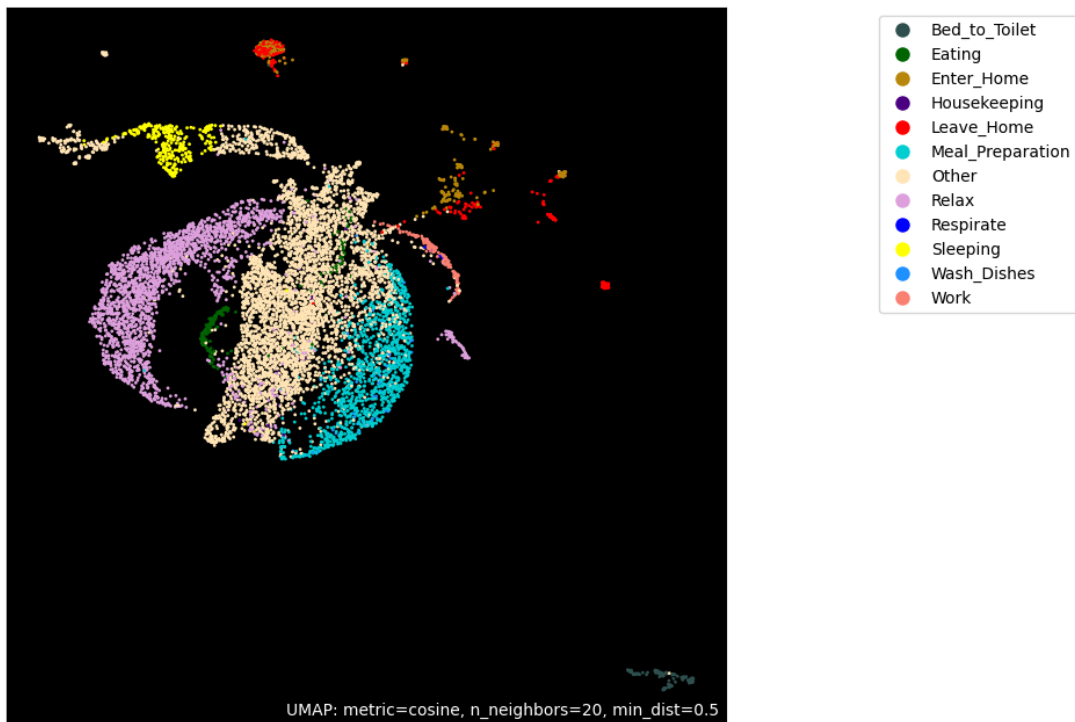
In this appendix, we present the embeddings of activities from three datasets: Aruba, Milan, and Cairo. These embeddings effectively capture the relationships between various activities and provide a visual representation of the feature space for each activity. We conduct a comparative analysis of the embeddings generated by the ELMo and GPT models. The left images in our figures showcase activities embedded using the ELMo models, while the right images illustrate those embedded by the GPT models.

To generate the embedding of activity sequences, each pre-segmented activity from the datasets is processed through the respective embedding model. The resulting output vectors are then averaged to produce a unique vector representation for each activity. Subsequently, these vectors are dimensionally reduced using the Uniform Manifold Approximation and Projection (UMAP) algorithm, enabling their representation in a 2-dimensional space. Each point in this space is color-coded according to its corresponding activity label. Figures 12, 13, and 14 demonstrate the ELMo-based and GPT-based activity sequence embeddings for the Aruba, Milan, and Cairo datasets, respectively.

We observe that the embeddings are generally similar. However, it is crucial to note that the GPT embedding is trained from random chunks that may not contain only one activity but potentially a sub-part or parts of multiple activities in contrary of ELMo which use pre-segmented activities. We can observe, in the Milan dataset, the GPT embedding appears to more distinctly separate some clusters, for instance, it isolate the 'master_bathroom' activities. For the Cairo dataset, the GPT embedding seems to segregate all activities into two main clusters: one grouping day activities and the other night activities.

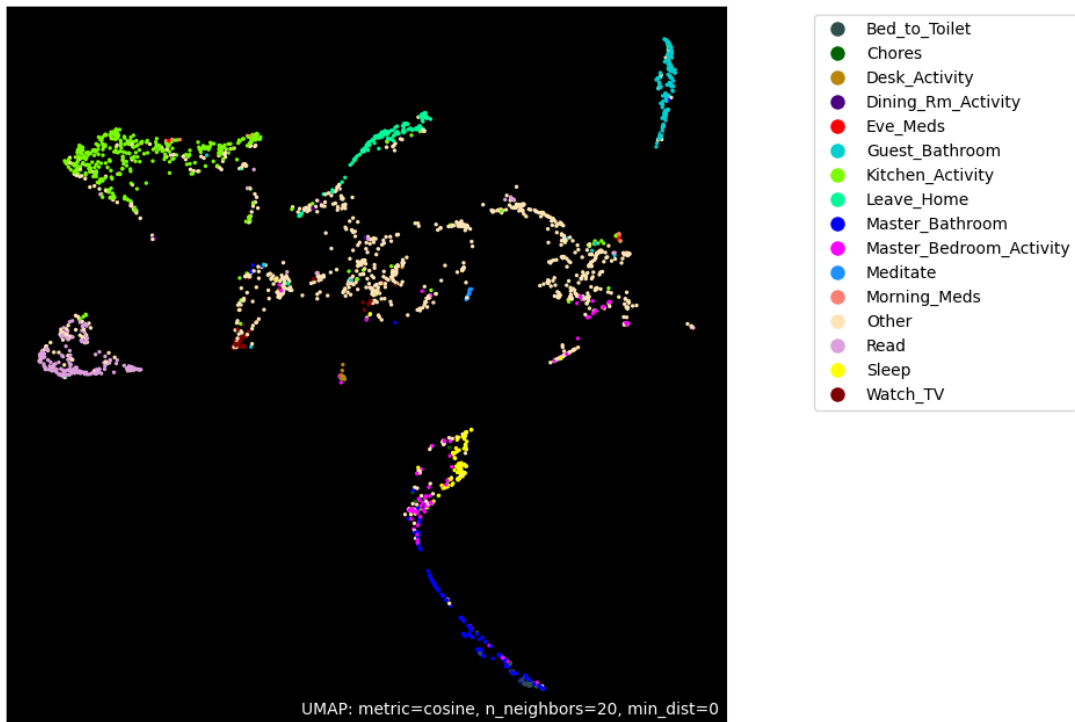


(a) ELMo

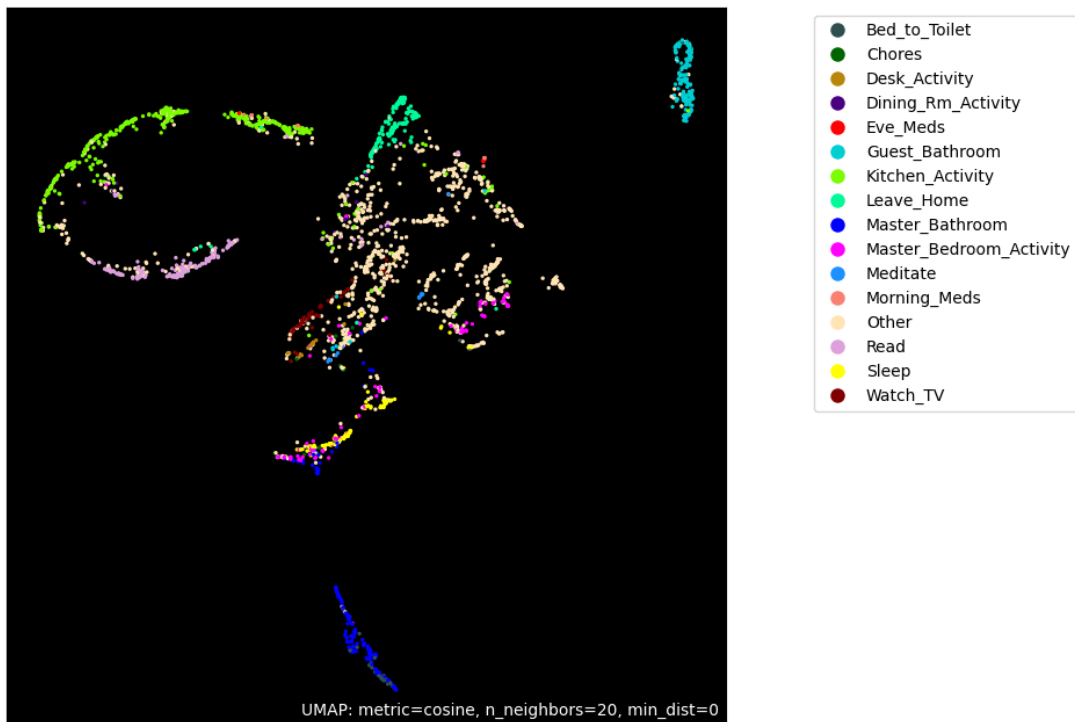


(b) GPT

Figure 12: Visualization of Activity Embeddings for the Aruba Dataset (Test Set) Generated by ELMo (Top) and GPT (Bottom)

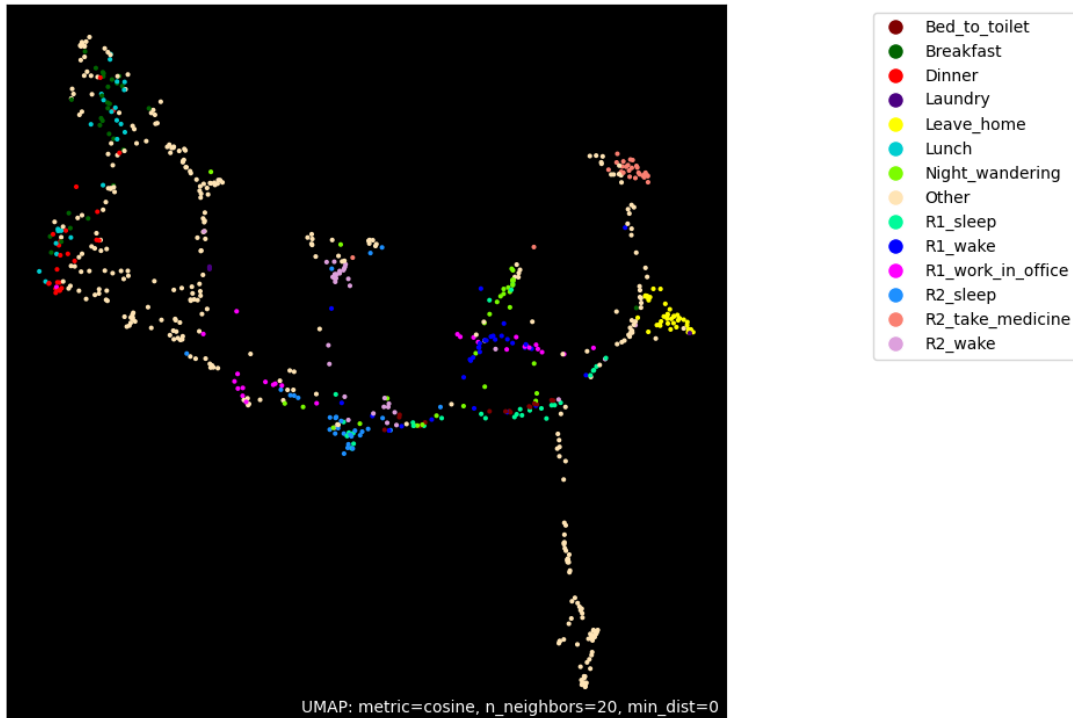


(a) ELMo

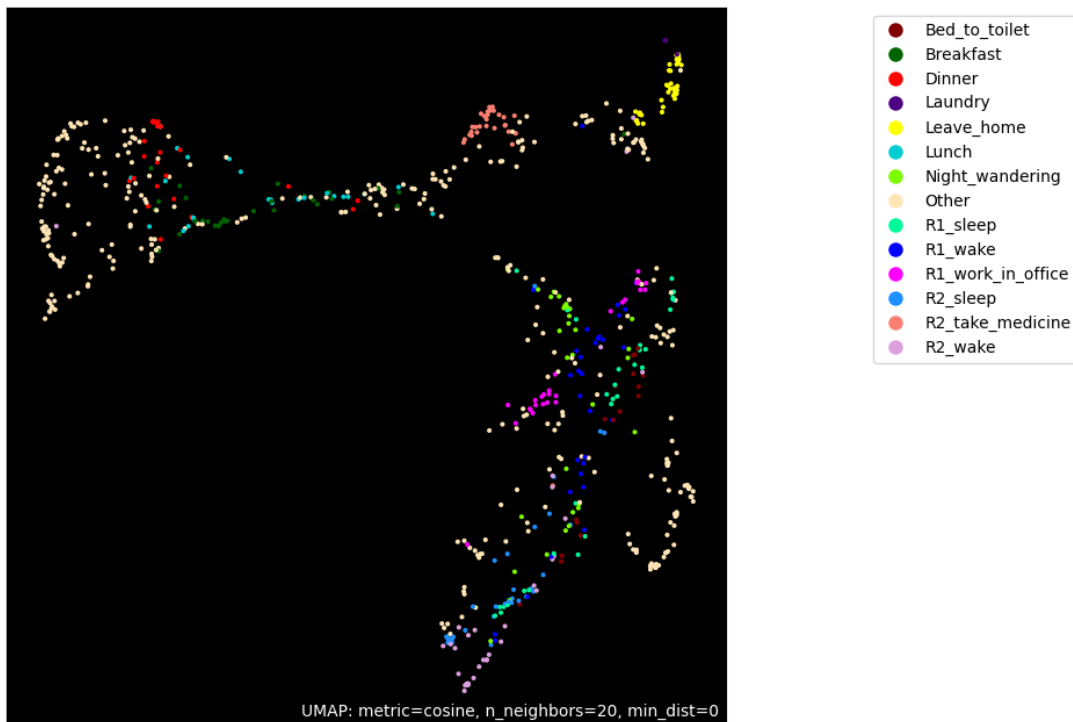


(b) GPT

Figure 13: Visualization of Activity Embeddings for the Milan Dataset (Test Set) Generated by ELMo (Top) and GPT (Bottom)



(a) ELMo



(b) GPT

Figure 14: Visualization of Activity Embeddings for the Cairo Dataset (Test Set) Generated by ELMo (Top) and GPT (Bottom)